ISSN 0021-3640, JETP Letters, 2017, Vol. 105, No. 2, pp. 98–102. © Pleiades Publishing, Inc., 2017.
Original Russian Text © I.S. Veshchunov, L.Ya. Vinnikov, V.S. Stolyarov, N. Zhou, Z.X. Shi, X.F. Xu, S.Yu. Grebenchuk, D.S. Baranov, I.A. Golovchanskiy, S. Pyon, Yue Sun, Wenhe Jiao, Guanghan Cao, T. Tamegai, A.A. Golubov, 2017, published in Pis'ma v Zhurnal Eksperimental'noi i Teoreticheskoi Fiziki, 2017, Vol. 105, No. 2, pp. 87–92.

CONDENSED MATTER

Visualization of the Magnetic Flux Structure in Phosphorus-Doped $EuFe_2As_2$ Single Crystals

I. S. Veshchunov[a, b], L. Ya. Vinnikov[c, *], V. S. Stolyarov[a, c], N. Zhou[d], Z. X. Shi[d], X. F. Xu[e], S. Yu. Grebenchuk[a], D. S. Baranov[a, c, f], I. A. Golovchanskiy[a, g], S. Pyon[b], Yue Sun[b, h], Wenhe Jiao[i], Guanghan Cao[i], T. Tamegai[b], and A. A. Golubov[a, j]

[a] *Moscow Institute of Physics and Technology (State University), Dolgoprudnyi, Moscow region, 141700 Russia*
[b] *Institute for Solid State Physics, The University of Tokyo, 277-8581 Kashiwa, Japan*
[c] *Institute of Solid State Physics, Russian Academy of Sciences, Chernogolovka, Moscow region, 142432 Russia*
[d] *Department of Physics and Key Laboratory of MEMS of the Ministry of Education, Southeast University, 211189 Nanjing, China*
[e] *Department of Physics, Changshu Institute of Technology, Changshu 215500, People's Republic of China*
[f] *Laboratoire de physique et d'etude des materiaux, LPEM-UMR8213/CNRS-ESPCI ParisTech-UPMC, 75005 Paris, France*
[g] *National University of Science and Technology MISIS, Moscow, 119049 Russia*
[h] *Department of Applied Physics, The University of Tokyo, 7-3-1 Hongo, Bunkyo-ku, Tokyo 113-8656, Japan*
[i] *Department of Physics, Zhejiang University, 310027 Hangzhou, China*
[j] *Faculty of Science and Technology and MESA+ Institute of Nanotechnology, University of Twente, 7500 AE Enschede, The Netherlands*
***** *e-mail: vinnik@issp.ac.ru*

Received November 30, 2016

Magnetic flux structure on the surface of $EuFe_2(As_{1-x}P_x)_2$ single crystals with nearly optimal phosphorus doping levels $x = 0.20$ and $x = 0.21$ is studied by low-temperature magnetic force microscopy and decoration with ferromagnetic nanoparticles. The studies are performed in a broad temperature range. It is shown that the single crystal with $x = 0.21$ in the temperature range between the critical temperatures $T_{SC} = 22$ K and $T_C = (18 \pm 0.3)$ K of the superconducting and ferromagnetic phase transitions, respectively, has the vortex structure of a frozen magnetic flux, typical for type-II superconductors. The magnetic domain structure is observed in the superconducting state below T_C. The nature of this structure is discussed.

DOI: 10.1134/S0021364017020151

The coexistence of superconductivity and magnetic ordering has been a subject of a strong interest [1]. Currently, the electric transport and magnetic properties are well studied for a number of single-crystalline compounds of the so-called magnetic superconductors: borocarbides [2], uranium compounds [3], high-temperature cuprate superconductors [4], and iron-based superconductors [5].

An important issue of the coexistence of superconductivity and magnetism from both theoretical [6, 7] and experimental perspectives [8] relates to the microstructure of the magnetic flux, as well as to its dynamics upon variation of the temperature and external magnetic field. Until recently, low temperatures of superconducting and magnetic phase transitions of known single crystals, as well as the requirement of a high spatial resolution, have limited experimental capabilities for visualization of the magnetic flux structure employing, e.g., magnetic force microscopy (MFM) [9] and decoration with magnetic nanoparticles [10]. Recently, new iron-based compounds $AFe_2(As_{1-x}P_x)_2$ (where A = Ba, Sr, Ca, Eu) have been synthesized. Superconductivity in these compounds can be induced by doping with phosphorus [11]. Superconductivity in $EuFe_2(As_{1-x}P_x)_2$ single crystals occurs in a rather narrow doping range $x = 0.14$–0.25 (or in the phosphorus content range 7.0–12.5 at %) with the maximum superconducting transition temperature $T_{SC}^{max} = 27$ K [12, 13]. The magnetic transition in the Eu^{2+} subsystem is observed at temperatures $T_C \sim 17$–20 K and depends moderately on the phosphorus content (doping level) in the specified range of content [12, 13]. Previously, the magnetic flux distribution was visualized with the MFM on artificial thin-film superconductor/ferromagnet (Nb/FeNi) hybrid structures [8], where domains and Abrikosov vortices

frozen in the superconductor were observed simultaneously. However, in [8], the Curie temperature T_C of ferromagnetic layers was much higher than the critical temperature of the superconducting transition T_{SC} in niobium films. Also, vortex structures were observed in spatially homogeneous $ErNi_2B_2C$ bulk superconducting single crystals ($T_{SC} = 10.5$ K) in [14] using the decoration method, and interpreted as an evidence of presence of domain boundaries in a weakly ferromagnetic phase with $T_C = 2.3$ K.

In this work, the magnetic flux structure in $EuFe_2(As_{1-x}P_x)_2$ single crystals with $x = 0.20$ and $x = 0.21$ is studied with the MFM and the Bitter decoration technique in a broad temperature range. Stripe and maze domain structures typical for ferromagnets with perpendicular magnetic anisotropy, are observed in the superconducting state below T_C. In contrast to artificial hybrid systems, in $EuFe_2(As_{1-x}P_x)_2$ an interface is absent and superconductivity and ferromagnetism coexist on the atomic scale.

$EuFe_2(As_{1-x}P_x)_2$ single crystals were synthesized using the self-flux method [15]. The actual composition of synthesized single crystals was determined by energy dispersive X-ray (EDX) microanalysis employing Carl Zeiss Supra 50 VP SEM microscope. For MFM and decoration studies, single crystals of $EuFe_2(As_{0.80}P_{0.20})_2$ and $EuFe_2(As_{0.79}P_{0.21})_2$ of $1\times1\times0.012$ mm^3 size with an atomically smooth surface were obtained by mechanical cleavage. Temperature and field dependences of the magnetization were measured on a Quantum Design MPMS-XL5 SQUID magnetometer in fields up to 5 T. The surface structure and the distribution of magnetic flux were studied using AttoCube AttoDry 1000 atomic force microscope (AFM) with a closed-cycle cryogenic system and a base temperature of 4 K. For AFM and MFM studies, silicon cantilevers were used coated by magnetic CoCr layer (MESP, Bruker) with the following characteristics at 4.2 K: the resonance frequency of the cantilever 87 kHz, the stiffness constant 2.8 N/m, and the coercive field ≈1400 Oe. AFM/MFM imaging was performed in an atmosphere of exchange gas (helium) at pressure $P \sim 0.5$ mbar in the temperature range from 4 to 30 K, controlled with exceptional precision of 1 mK. Prior to MFM imaging, probes were magnetized at $H = 2$ kOe above the superconducting transition temperature $T_{SC} = 22$ K of the $EuFe_2(As_{0.79}P_{0.21})_2$ sample. The topography of the surface was studied in the tapping mode and the magnetic flux structure was imaged in the MFM lift mode at 110 nm above the sample surface with the feedback switched off and fast scanning direction along the Y axis. The MFM contrast was provided by the phase shift in the cantilever oscillation. The decoration of the surface of $EuFe_2(As_{0.80}P_{0.20})_2$ single crystal was performed with magnetic iron particles (~10 nm) in the field cooling (FC) regime at liquid helium temperatures [10].

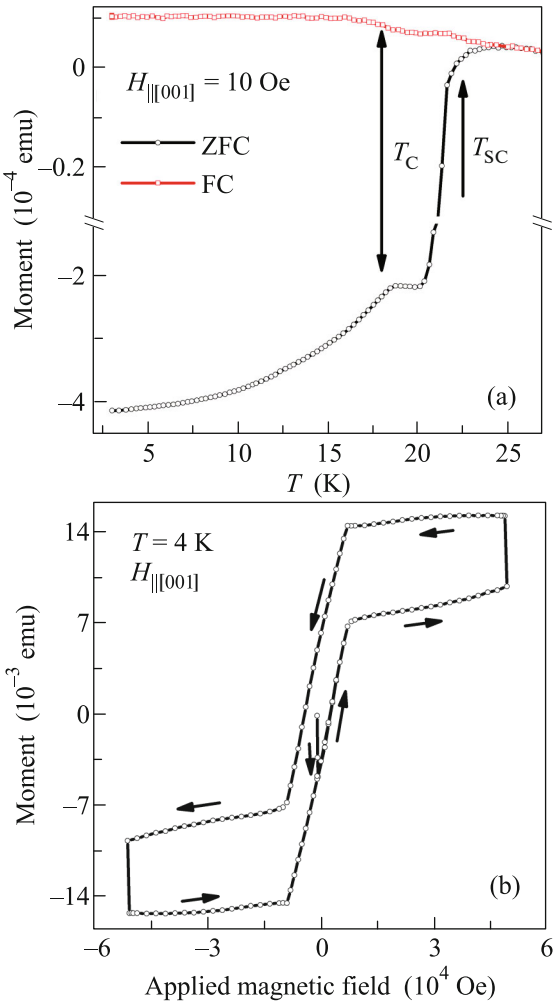

Fig. 1. (Color online) Temperature dependence of the magnetization and magnetization curve for $EuFe_2(As_{0.79}P_{0.21})_2$ single crystal. (a) Temperature dependence of the magnetization measured in the FC regime with the field parallel to the **c**-axis of the crystal and in the zero-field cooling (ZFC) regime. Transitions to the superconducting and ferromagnetic states are observed at $T_{SC} = 22$ K and $T_C = (18 \pm 0.3)$ K, respectively (marked by arrows). (b) The dependence of the magnetization on the applied magnetic field at $T = 4$ K.

Figure 1 shows typical magnetic properties of $EuFe_2(As_{0.79}P_{0.21})_2$ single crystal. Figure 1a demonstrates the temperature dependences of the magnetization measured in the FC and zero-field cooling (ZFC) regimes. The superconducting transition temperature $T_{SC} = 22$ K is indicated by the right arrow. Step features on the ZFC and FC temperature dependences of the magnetization are attributed to a ferromagnetic phase transition. It is noteworthy that a transition to the superconducting state is also accompanied by the appearance of residual magnetization upon cooling in

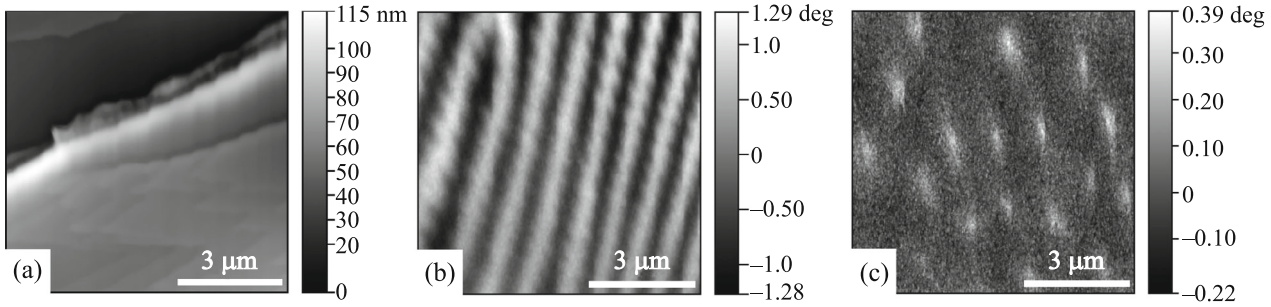

Fig. 2. AFM topographic image and MFM images of magnetic flux structure on the (001) surface of $EuFe_2(As_{0.79}P_{0.21})_2$ single crystal. (a) AFM topography of the surface area in fully magnetized state of the Eu^{2+} ferromagnetic subsystem in magnetic field of $H = -0.9$ T parallel to the **c**-axis. (b) Magnetic domain structure after zero-field cooling down to the minimum temperature $T_{min} = 4.16$ K with subsequent heating up to $T = 17.27$ K. (c) Vortex structure imaged after FC at $T = 18.15$ K with the residual magnetic flux density $\Phi_0/a^2 \sim 6$ G.

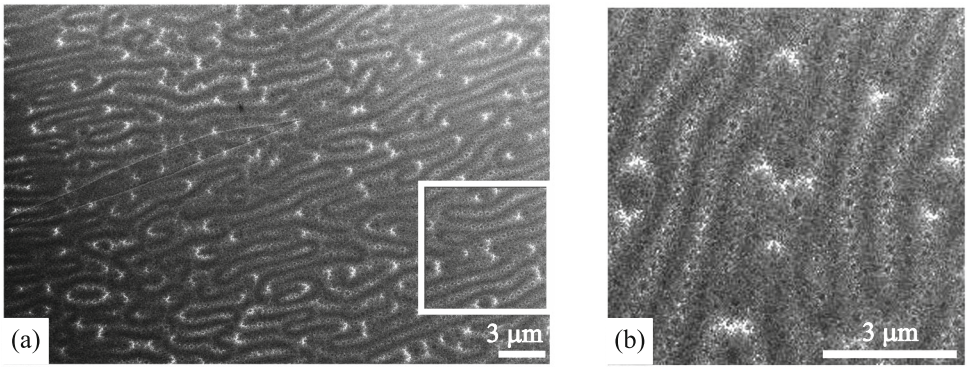

Fig. 3. (a) Magnetic flux structure on the (001) surface of $EuFe_2(As_{0.80}P_{0.20})_2$ single crystal after FC in a magnetic field of 10 Oe revealed by decoration at $T_d \sim 8$ K. (b) Enlarged image of the area indicated by the white box in (a) of similar size and the orientation of the domain structure shown in Fig. 2b.

an external field of 10 Oe. Figure 1b shows the dependence of the magnetization on the applied magnetic field parallel to the **c**-axis of the crystal. For the sample with $x = 0.20$, the temperature dependence of the magnetization and magnetization curve at 4 K are similar but with a higher superconducting transition temperature and a wider hysteresis loop.

Figure 2 shows the results of the AFM/MFM studies. Figure 2a demonstrates the AFM topography of the 8×8-μm^2 surface area of $EuFe_2(As_{0.79}P_{0.21})_2$ single crystal with the step of ~100 nm height. Figure 2b shows the distribution of the magnetic flux over the surface shown in Fig. 2a at $T = 17.27$ K. This structure is typical for the entire temperature range below the Curie temperature and disappears after heating above T_C. Thus, the observed sign-alternating contrast can be attributed to the magnetic domain structure. Importantly, the domain structure is observed not only at zero external magnetic field but also upon cooling in weak fields $H < 100$ Oe. Figure 2c shows the distribution of the magnetic flux in the superconducting state in a narrow temperature range above T_C. The observed contrast (light spots) corresponds to Abrikosov vortices with the magnetic flux density $\Phi_0/a^2 \sim 6$ G, where Φ_0 is the magnetic flux quantum and a is the average distance between vortices.

Figure 3 shows the typical magnetic flux structure observed by the decoration method on the (001) surface of $EuFe_2(As_{0.80}P_{0.20})_2$ single crystal with the superconducting transition temperature $T_{SC} = 24$ K. With MFM, only a small ~8×8-μm^2 surface area of the sample was studied, whereas the decoration method reveals the magnetic structure on the almost entire surface. According to the principle of the image contrast formation in the decoration method [16, 17], the region of higher density of magnetic particles (light) is treated as a domain with the magnetization along the applied field direction, whereas the region with lower density or without magnetic particles

(dark) is interpreted as a domain with the opposite sign of the magnetization. As can be seen, the decorated domain structure (Fig. 3b) agrees with MFM imaged one (Fig. 2b) at corresponding scales. The period of the domain structure is about 0.9 μm. At the same time, finer details of the decorated domain structure can be resolved (Fig. 3b). The magnetization measurements and both MFM imaged and decorated magnetic structure define explicitly $EuFe_2(As_{0.79}P_{0.21})_2$ and $EuFe_2(As_{0.80}P_{0.20})_2$ single crystals as superconductors with ferromagnetic ordering and the superconducting transition temperature T_{SC} above the Curie temperature T_C.

The experimental results can be interpreted as follows. According to the dependences shown in Fig. 1a, the ZFC magnetization is negative below the superconducting transition temperature $T_{SC} = 22$ K. In the temperature range below T_C, the diamagnetic response is weakened by the ferromagnetic transition in the Eu^{2+} subsystem. The exact determination of the Curie temperature using the observed features on the ZFC and FC temperature dependences of the magnetization is complicated due to competing mechanisms of superconducting and ferromagnetic orderings. In particular, maxima on the FC and ZFC temperature dependences of the magnetization are observed in [12] at $T \sim 17.7$ K, whereas according to measurements of the specific heat, the Curie temperature is $T_C = 19$ K. In this work, the transition temperature to the ferromagnetic state T_C is defined as a temperature at which the domain structure is first observed; i.e., $T_C =$ 17.7 K. The dependence of the magnetization on the applied magnetic field (Fig. 1b) is the superposition of a typical hysteresis loop of a type-II superconductor (within the Bean model the critical current density J_c is proportional to the width of the hysteresis loop) and the magnetization curve of the Eu^{2+} ferromagnetic subsystem [12].

The magnetic origin of the domain structure contrast (Figs. 2b and 3a) is confirmed by insensitivity of the MFM probe to small details of the surface topography, e.g., to the 100 nm step. Sign-alternating (phase) contrast on domains indicates perpendicular magnetic anisotropy and corresponds to the antiparallel direction of the magnetization in neighboring domains.

Individual vortices could not be resolved with decoration since the expected magnetic flux density within domains is about 0.9 T ($M_s = 714$ cgs units/cm^3) at liquid helium temperatures [12], whereas the resolution of the decoration method is limited by 0.2 T [18]. The spatial resolution of MFM also cannot identify individual vortices if the local magnetic flux density in domains is much higher than 10 mT [19]. At the same time, the fine structure of domains, which is shown in Fig. 3b, can be explained within the framework of domain branching in ferromagnets [20]. An alternative origin of the fine domain structure is the so-called intermediate-mixed state [21], which appears if the thickness of the superconducting crystal is much larger than the width of domains and is characterized by a mixture of flux-free domains (Meissner phase) and domains with Abrikosov vortices. In contrast to the structure of the intermediate-mixed state, the fields of vortices in neighboring branching domains should be oppositely oriented. Such a possibility was theoretically considered in [7]. According to this model, different types of domain configurations can be formed in a ferromagnetic superconductor depending on the parameters (magnetic and superconducting): the saturation magnetization (M_s), the London penetration depth (λ), the lower critical field (H_{c1}), and the domain wall width w. Precise measurements of these parameters and studies of the fine structure of domains will provide further clarification of the mechanisms of the coexistence and mutual effect of superconductivity and ferromagnetism in studied single crystals.

The main result of this work is the observation of the magnetic domain structure in $EuFe_2(As_{1-x}P_x)_2$ superconducting single crystals with $x = 0.20$ and $x = 0.21$. This domain structure disappears in $EuFe_2(As_{0.79}P_{0.21})_2$ single crystal after heating above the Curie temperature $T_C = 17.7$ K. Thus, the magnetic domain structure has been observed for the first time in spatially homogeneous single crystals with $T_{SC} > T_C$, which unambiguously indicates the coexistence of ferromagnetism and superconductivity in this material.

The observations of the magnetic flux structure using low-temperature MFM and decoration methods in real space (in contrast to X-ray and neutron diffraction studies) provide important information on the topology, real sizes, and shape of domains. At the same time, only further combined studies employing, e.g. diffraction methods and scanning probe microscopy, in particular, high-resolution scanning tunneling microscopy, as well as decoration with ferromagnetic nanoparticles in a broad range of temperatures and magnetic fields, can clarify the mechanism of the coexistence of superconductivity and ferromagnetism in $EuFe_2(As_{1-x}P_x)_2$ ferromagnetic superconductors.

I.S.V., L.Ya.V., and V.S.S. are grateful to V.V. Ryazanov, L.S. Uspenskaya, S.I. Bozhko, and A.I. Buzdin for stimulating discussions. We are grateful to V.V. Dremov, E.Yu. Postnova, A.G. Shishkin, and L.G. Isaeva for assistance. N.Z., Z.X.S., X.F.X., W.J., and G.C. acknowledge the support by the National Science Foundation of China (no. 11474252, 11611140101, and U1432135). The work of V.S.S., D.S.B., and I.A.G. was supported by the Russian Foundation for Basic Research (project nos. 16-32-60133 mol-a-dk and 16-32-00309 mol-a). MFM stud-

ies were supported by the Ministry of Education and Science of the Russian Federation (project no. 14.Y26.31.0007).

REFERENCES

1. A. D. Huxley, Physica C **514**, 368 (2015); C. T. Wolowiec, B. D. White, and M. B. Maple, Physica C **514**, 113 (2015).
2. L. C. Gupta, Adv. Phys. **55**, 691 (2006).
3. N. T. Huy, A. Gasparini, D. E. de Nijs, Y. Huang, J. C. P. Klaasse, T. Gortenmulder, A. de Visser, A. Hamann, T. Görlach, and H. V. Löhneysen, Phys. Rev. Lett. **99**, 067006 (2007); D. Aoki, A. Huxley, E. Ressouche, D. Braithwaite, J. Flouquet, J.-P. Brison, E. Lhotel, and C. Paulsen, Nature (London) **413**, 613 (2001); D. J. Hykel, C. Paulsen, D. Aoki, J. R. Kirtley, and K. Hasselbach, Phys. Rev. B **90**, 184501 (2014).
4. A. N. Lavrov, L. P. Kozeeva, M. R. Trunin, and V. N. Zverev, Phys. Rev. B **79**, 214523 (2009).
5. Y. Kamihara, T. Watanabe, M. Hirano, and H. Hosono, J. Am. Chem. Soc. **130**, 3296 (2008).
6. T. K. Ng and C. M. Varma, Phys. Rev. Lett. **78**, 330 (1997); E. I. Blount and C. M. Varma, Phys. Rev. Lett. **42**, 1079 (1979).
7. M. Fauré and A. I. Buzdin, Phys. Rev. Lett. **94**, 187202 (2005); I. M. Khaymovich, A. S. Mel'nikov, and A. I. Buzdin, Phys. Rev. B **89**, 094524 (2014).
8. M. Iavarone, A. Scarfato, F. Bobba, M. Longobardi, G. Karapetrov, V. Novosad, V. Yefremenko, F. Giubileo, and A. M. Cucolo, Phys. Rev. B **84**, 024506 (2011); F. Bobba, C. di Giorgio, A. Scarfato, et al., Phys. Rev. B **89**, 214502 (2014).
9. D. Wulferding, I. Yang, J. Yang, M. Lee, H. C. Choi, S. L. Bud'ko, P. C. Canfield, H. W. Yeom, and J. Kim, Phys. Rev. B **92**, 014517 (2015).
10. L. Ya. Vinnikov, I. V. Grigor'eva, and L. A. Gurevich, Springer Ser. Mater. Sci. **23** (1993).
11. Z. Ren, Q. Tao, S. Jiang, C. M. Feng, C. Wang, J. H. Dai, G. H. Cao, and Z.-A. Xu, Phys. Rev. Lett. **102**, 137002 (2009).
12. H. S. Jeevan, D. Kasinathan, H. Rosner, and P. Gegenwart, Phys. Rev. B **83**, 054511 (2011); S. Nandi, W. T. Jin, Y. Xiao, Y. Su, S. Price, D. K. Shukla, J. Strempfer, H. S. Jeevan, P. Gegenwart, and Th. Bruckel, Phys. Rev. B **89**, 014512 (2014).
13. T. Adachi, Y. Nakamatsu, T. Kobayashi, S. Miyasaka, S. Tajima, M. Ichimiya, M. Ashida, H. Sagayama, H. Nakao, R. Kumai, and Y. Murakami, J. Phys. Soc. Jpn. **85**, 063705 (2016).
14. I. S. Veschunov, L. Ya. Vinnikov, S. L. Bud'ko, and P. C. Canfield, Phys. Rev. B **76**, 174506 (2007).
15. X. Xu, W. H. Jiao, N. Zhou, Y. K. Li, B. Chen, C. Cao, J. Dai, A. F. Bangura, and G. H. Cao, Phys. Rev. B **89**, 104517 (2014).
16. I. S. Veshchunov, V. A. Oboznov, A. N. Rossolenko, A. S. Prokofiev, L. Ya. Vinnikov, A. Yu. Rusanov, and D. V. Matveev, JETP Lett. **88**, 758 (2008).
17. T. Sakurai and Y. Shimada, Jpn. J. Appl. Phys. **31** (6A), 1905 (1992).
18. L. Ya. Vinnikov, T. L. Barkov, P. C. Canfield, S. L. Bud'ko, J. E. Ostenson, F. D. Laabs, and V. G. Kogan, Phys. Rev. B **64**, 220508(R) (2001).
19. A. Volodin, K. Temst, C. Van Haesendonck, Y. Bruynseraede, M. I. Montero, and I. K. Schuller, Europhys. Lett. **58**, 582 (2002).
20. A. Hubert and R. Schäfer, *Magnetic Domains. The Analysis of Magnetic Microstructures* (Springer, Berlin, Heidelberg, New York, 1998); L. D. Landau and E. M. Lifshitz, *Course of Theoretical Physics,* Vol. 8: *Electrodynamics of Continuous Media* (Nauka, Moscow, 1982; Pergamon, Oxford, 1984).
21. A. O. Golubok and L. Ya. Vinnikov, JETP Lett. **35**, 642 (1982).